Available online at www.sciencedirect.com
ScienceDirect
Journal of Power Sources 160 (2006) 105–115
JOURNAL OF POWER SOURCES
www.elsevier.com/locate/jpowsour

Control of methanol transport and separation in a DMFC with a porous support

Nobuyoshi Nakagawa*, Mohammad Ali Abdelkareem, Kazuya Sekimoto

Department of Biological and Chemical Engineering, Gunma University, 1-5-1 Tenjin, Kiryu, Gunma 375-8501, Japan

Received 5 January 2006; received in revised form 22 January 2006; accepted 24 January 2006
Available online 28 February 2006

Abstract

The effect of porous support properties such as porosity ε and water absorptivity α_w on the methanol crossover (MCO) and transport phenomena through the membrane electrode assembly (MEA) of a direct methanol fuel cell (DMFC) under open circuit conditions was theoretically and experimentally investigated. Porous plates, made of different materials, with different properties, were used as the support of the DMFC, and the performance of the crossover, i.e., CO_2 production rate at the cathode, cell temperature, fluxes of water and methanol, through the MEA with or without the porous plate were measured and compared to each other. The methanol flux increased with the increasing product of ε and α_w, $\varepsilon\alpha_w$, and the water flux slightly decreased with its increase, in the range where $\varepsilon\alpha_w$ was over a certain value, suggesting that the methanol flux was controlled by the diffusion resistance through the porous plate, whereas the total flux was not affected by it. It was clearly shown that these porous plates prevented the passive DMFC from undergoing a significant loss of methanol due to the crossover, and also being out of temperature control.

Keywords: Passive DMFC; Methanol crossover; Porosity; Water absorptivity; Cell temperature; Porous plate

1. Introduction

There has been a increasing demand for the development of direct methanol fuel cells (DMFCs) [1–3] because of their high energy densities which are suitable for mobile electric devices and automobiles. However, the energy density of the DMFCs currently under development is still far from that expected due to the methanol crossover and the high overvoltage at the electrodes [4,5]. Due to the methanol crossover, the DMFC usually shows the highest performance at low concentrations of methanol from 2 to 3 M [6,7] under the active conditions. To overcome the methanol crossover, a large number of studies [8–12] were carried out for developing a new proton-conducting membrane with a low methanol permeability and high proton conductivity. Modification of the existing membranes like Nafion has also been conducted by making it a composite membrane [13–15] with inorganic or organic materials, surface modification by physical treatment [16] or by coating the surface with a thin film [17–19]. Only a few papers considered the reducing ability in methanol crossover by mass transport control in the backing layer [20,21].

Recently, passive DMFCs, that suck methanol from a reservoir by an osmotic action and breath air from its surrounding by natural convection and diffusion, have been demonstrated, and the performance was investigated by some researchers under different conditions [20,22–32]. The reports on the passive DMFCs revealed some different performance behaviors compared to that of active DMFCs. For example, a methanol concentration like 5 M, which is higher than that for an active DMFC, was sometimes assigned as the optimum condition for the *i*–*V* performance [18,27,33]. An air-breathing DMFC with a thinner membrane exhibited a better *i*–*V* performance at low current density [34]. The power density calculated on the basis of the unit area of the electrode for a stack was much better than that of the single cell [23]. A passive vertically oriented DMFC always produced a better performance than that horizontally oriented [35]. These behaviors were attributed to the methanol crossover that induced an increase in the cell temperature due to the exothermic reaction between the permeated methanol and the oxygen at the cathode, so that the polarization was reduced, and hence, a high performance was achieved [23,34,35]. These do not suggest that the methanol crossover played a desirable role in the passive DMFC.

* Corresponding author. Tel.: +81 277 30 1458; fax: +81 277 30 1457.
E-mail address: nakagawa@bce.gunma-u.ac.jp (N. Nakagawa).

0378-7753/$ – see front matter © 2006 Elsevier B.V. All rights reserved.
doi:10.1016/j.jpowsour.2006.01.066

It should be noted that the methanol crossover causes a loss of the methanol and significantly reduced the energy density and the efficiency of the DMFC. In the passive DMFCs, the methanol crossover and the temperature of the cell were not controlled, which sometimes leads to fatal damage to the cell.

The authors demonstrated, in a recent report [20], that a passive DMFC with a porous carbon plate as a support reduced the methanol crossover and constantly controlled the cell temperature. In the experiment, two different types of porous carbon plates were used, and their methanol crossover reductions were different suggesting that the properties of the porous plate affected the methanol crossover. The mechanism of reducing the MCO was explained by the diffusion control of the methanol through the porous plate. This study is primarily focused on a theoretical consideration for the reduction of the methanol crossover through the MEA with a porous plate. The behavior of the transport and separation of methanol through this type of passive DMFC under open circuit conditions was then investigated. Experiments were conducted to show the unique properties of this cell by measurement of the MCO using different porous materials, i.e., porous carbon and porous alumina, with different properties, e.g., pore structures, water absorptivity, at different methanol concentrations and different temperatures.

2. Theoretical consideration of the mass transfer through MEA

2.1. Mass flow rate of the solution

When an MEA with a polymer electrolyte membrane like Nafion is in contact with a methanol solution and air at both surfaces, the crossover of methanol and also water occurs. The mass flow rate of the solution M_T, a mixture of methanol and water, through the MEA would be controlled by the rate of removal of the solution from the cathode surface into the cathode gas due to vaporization under open circuit conditions, in some cases. The driving force of the vaporization is the difference in vapor pressure of the solution between the cathode surface and the flowing gas and the rate of vaporization, v_1, can be expressed as follows:

$$v_1 = k(p_v - p_a) \tag{1}$$

$$= k\,(p_0 \exp(-L_a/(RT)) - p_a) \tag{2}$$

where k is a constant, p_v the vapor pressure of the solution at the meniscus of the porous cathode, p_a the vapor pressure of the cathode gas, p_0 the vapor pressure of the bulk solution, and L_a is the latent heat of vaporization of the solution. Eq. (2) was derived from the Clausuis–Clapeyron relation.

The solution that exists at the cathode was a mixture of methanol and water, and the total flux across the membrane J_T consists of a methanol flux J_M and a water flux J_W:

$$J_T = J_M + J_W \tag{3}$$

and also, as the total flux is controlled by the rate of vaporization, and hence:

$$J_T = M_T/A = v_1/A \tag{4}$$

where A is the area of the membrane. The methanol flux can be related to the water flux based on the general relationship in flux between a solute and a solvent that permeate through a membrane as follows:

$$J_M = (1-\sigma)C_m^* J_W - D_{mM}(dC_m/dx) = J_{CM} + J_{DM} \tag{5}$$

The first term of Eq. (5) is the convection flux of methanol J_{CM} with the water flux and the second term shows the diffusion flux of methanol J_{DM}, where σ is the reflection coefficient, and C_m^* is the average concentration of methanol in the membrane and D_{mM} is the diffusion coefficient of methanol in the membrane, and C_m is the methanol concentration at position x in the membrane from the surface.

Methanol that usually permeated to the cathode is oxidized by oxygen into water with the help of a catalyst, and the methanol concentration at the cathode surface remained low. Under this situation, the diffusion flux, J_{DM} is increased by the increase of difference in the methanol concentration between both surfaces of the membrane. This raised the methanol flux J_M, while the total flux was constant, i.e., reducing the flux of water, because the total flux was controlled by the rate of water vaporization as shown by Eqs. (3) and (4). As a result, methanol preferentially permeated through the membrane, and this caused a significant loss in energy density and energy efficiency of the DMFC.

2.2. Methanol diffusion through a porous plate

Let us now consider a case where a porous plate, which absorbs water into the body by osmotic action, is used as a support of the MEA on the anode side. When the flow rate of the solution through the MEA driven by the evaporation of water at the cathode is not very high, the porous plate is not a resistance for the transport of the total solution through the porous plate and MEA, if the porous plate absorbs sufficient water. In addition, the flux of methanol through the membrane can be controlled by the diffusion resistance of the porous plate. This mechanism can reduce the diffusion flux of methanol through the membrane J_{DM} by reducing the methanol concentration at the anode surface resulting in reducing the difference in the methanol concentration between the surfaces of the membrane. The diffusion flux of methanol controlled by the porous plate can be given by Fick's law as follows:

$$J_{DM} = -D_{eff,M}(\Delta C_M/\Delta X) \tag{6}$$

where $D_{eff,M}$ is the effective diffusion coefficient of methanol through the porous plate, and ΔC_M is the difference in the concentrations of methanol between both sides of the porous plate with thickness ΔX.

The effective diffusion coefficient $D_{eff,M}$ depends on the properties of the porous plate where the coefficient is proportional to the porosity of cross-section ε_s and inversely proportional to the tortosity τ of the porous plate as follows:

$$D_{eff,M} = kD_M\varepsilon_s/\tau \tag{7}$$

where D_M is the diffusion coefficient of methanol in water and k is a constant related to the affinity between methanol and the surface of the porous material.

When some pores are filled with the methanol–water solution due to the hydrophilic properties of the porous plate and the diffusion through the flooded pore dominates the mass transport, Eq. (7) can be modified as follows:

$$D_{\mathrm{eff,M}} = k' D_M (\alpha_s \varepsilon)^{2/3}/\tau \quad (8)$$

where α_s is the absorptivity of the solution to the porous plate defined by the volume fraction of flooded pore to that of the total pore, and ε is the porosity in volume. The power 2/3 in the equation expresses the transfer in the cross-sectional value instead of the volumetric value.

For a methanol–water solution, the absorptivity of solution α_s can be empirically related to that of water α_w due to the change in the surface tension:

$$\alpha_s = k_1 + k_2 \alpha_w \quad (9)$$

where k_1 and k_2 are the constants depending on the methanol concentration and type of porous material.

Based on the above mechanism, the methanol flux through the MEA and the acceleration effect on it can be reduced by the porous plate. In the following sections, the mechanism will be experimentally confirmed.

3. Experimental

3.1. Measurements of the pore structure and the water absorptivity of the porous plates

The porous plates used as the MEA support in this study included seven different types of porous carbon plates supplied from Mitsubishi Pencil Co., Ltd., and one Al_2O_3 porous plate from Nikkato Co., Ltd., used as a membrane in the electrolysis. The properties and pore structure of this porous plate are listed in Table 1. The porous carbon plates were categorized into two types, the CS type that was made of graphitic carbon and amorphous carbon and the CY type that was made of amorphous carbon. The Al_2O_3 porous plate, denoted as CER, was prepared as a reference to check if the carbon material is significantly important for controlling the MCO.

Table 1
Properties of the carbon paper and the porous carbon plates used

Anode backing	δ (mm)	α_w	Pore structure measured by the mercury porosimeter		
			V_p (cm^3 g^{-1})	$d_{p,ave}$ (μm)	ε
C-paper	0.17	0.82	1.51	50.6	0.81
CS1	2.0	0.0	0.137	2.0	0.244
CS2	2.0	0.15	0.521	2.0	0.487
CS3	2.0	0.55	0.248	2.0	0.33
CS4	2.0	0.9	–	2.0	0.49
CS5	2.0	0.83	0.265	7.8	0.43
CY1	2.0	0.5	–	20	0.59
CY2	2.0	0.7	0.775	43.8	0.588
CER	2.0	0.87	0.129	0.4	0.322

δ: thickness; α_w: water absorptivity defined by Eq. (7); V_p: total cumulative volume; d_p: pore diameter; ε: total porosity.

The microstructure of the porous plates was measured using a mercury porosimeter, Pascal 140 + 440 (Thermo Finnigan, Inc.). The water absorptivity, α_w, was defined as the fraction of the pore volume that filled with water when the plate was dipped into water for a long enough time. In the table, the properties and pore structure of a conventional carbon paper, C-paper, is also listed for comparison. It was clear that the porous carbon plates had a smaller average-pore diameter and porosity than that of the carbon paper.

The water absorptivity α_w of the porous plates combined with the porous plate cut into a 10 mm wide, 50 mm long and 2 mm thick strip by fully immersing the stick in water until its weight became constant. From the volume of the initial pore, V_0, and the volume of the absorbed water, V_w, the absorptivity was calculated as follows:

$$\alpha_w = V_w / V_0 \quad (10)$$

3.2. MEA preparation

3.2.1. Conventional MEA

The conventional MEA, which uses carbon paper as the anode-backing layer, was prepared in the following manner. Catalyst ink containing Pt–Ru (54 wt.%, Pt/Ru = 1.5)/C catalyst, a 5 wt.% Nafion solution (Wako, Inc.) and glycerol in the weight ratio of 1:3:3 was applied on the carbon paper (TGP-H-060, Toray, Inc.) to give a catalyst loading of 3–4 mg cm^{-2} and then used as the anode after being dried in a vacuum oven for 3 h. A ready-made electrode, EC-20-10 (ElectroChem, Inc.) with Pt (1.0 mg cm^{-2})/C was used as the cathode. Nafion 112 was used as the electrolyte membrane. It was pretreated to activate the proton conduction as follows: dipping it into 3 vol.% H_2O_2, de-ionized water, 2.5 mol dm^{-3} H_2SO_4 and de-ionized water in that order and boiling each solution for 1 h during each step. Finally, the MEA was fabricated by sandwiching the membrane between the anode and the cathode and hot pressing them at 403 K and 9 MPa for 3 min. The conventional MEA was labeled as MEA_C in this paper.

3.2.2. MEA with the porous plate

The porous plate was cut into a 10 mm wide, 50 mm long and 2 mm thick strip and was used as the support of the cell, i.e., used as an anode backing instead of the carbon paper for the conventional MEA. In a preliminary experiment, we confirmed that the mass transport through the MEA with a porous plate was unrelated between the case where the porous plate was mated with the membrane by hot pressing and the case where the porous plate was just placed on the conventional MEA. Hence, we put the porous plate on the anode surface of the conventional MEA and fixed them by pressing them in the cell holder. Therefore, the porous plate acted as a barrier to mass transport between the methanol reservoir and the anode surface. These MEAs with the porous plate was denoted

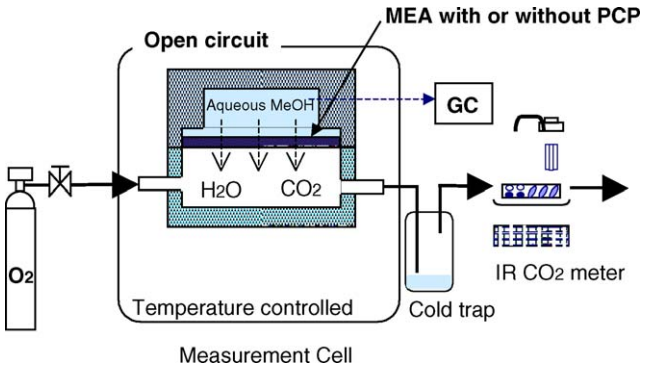

Fig. 1. Experimental apparatus used for measuring the methanol crossover under open circuit conditions.

as MEA/CSi or MEA/CYi depending on the type of porous plate.

3.3. Methanol and water flux measurements

Fig. 1 shows the experimental setup used to measure the mass transport through the MEA with or without the porous plate. The MEA with or without the porous plate was placed on a holder as shown in the figure. The cell chamber was separated by the MEA into the methanol reservoir and the oxygen flow chamber, and it arranged such that the reservoir top and the oxygen chamber bottom remained in constant contact between the solution and MEA. Into the oxygen chamber, the oxygen gas flowed at 500 ml min^{-1} from a cylinder. On the other hand, the CO_2 produced in the oxygen chamber by the oxidation of methanol permeated from the reservoir with the help of the Pt catalyst in the gas exhaust was measured using the IR CO_2 meter. In a preliminary experiment, we found, under certain conditions of this study, that 85–90% of the permeated methanol was converted to CO_2 and 10–15% of the permeated methanol was not completely oxidized. Hence, the CO_2 production rate was used to determine a trend in the time profile of the methanol crossover rate. We also measured the weight loss of the entire cell holder at a certain time interval and the methanol concentration of the liquid that remained in the reservoir after the experiment. The total flux was calculated from the weight loss, and the methanol flux was calculated from the amount of the methanol consumed from the reservoir during the experiment. The water flux was also calculated by subtracting the methanol flux from the total flux. These fluxes were the time average value in the 4 h experiment.

3.4. Controlling and measuring the temperature of the cell

The entire cell holder was placed it in a furnace and the surrounding temperature was adjusted at the desired temperature by the furnace. The holder was kept for sufficient time until the entire holder reached to the desired temperature before the measurement. The surrounding temperatures employed in this study were 297, 310 and 323 K.

In some experiments, the temperature of the cell was directly measured using a thermocouple placed on the cathode surface.

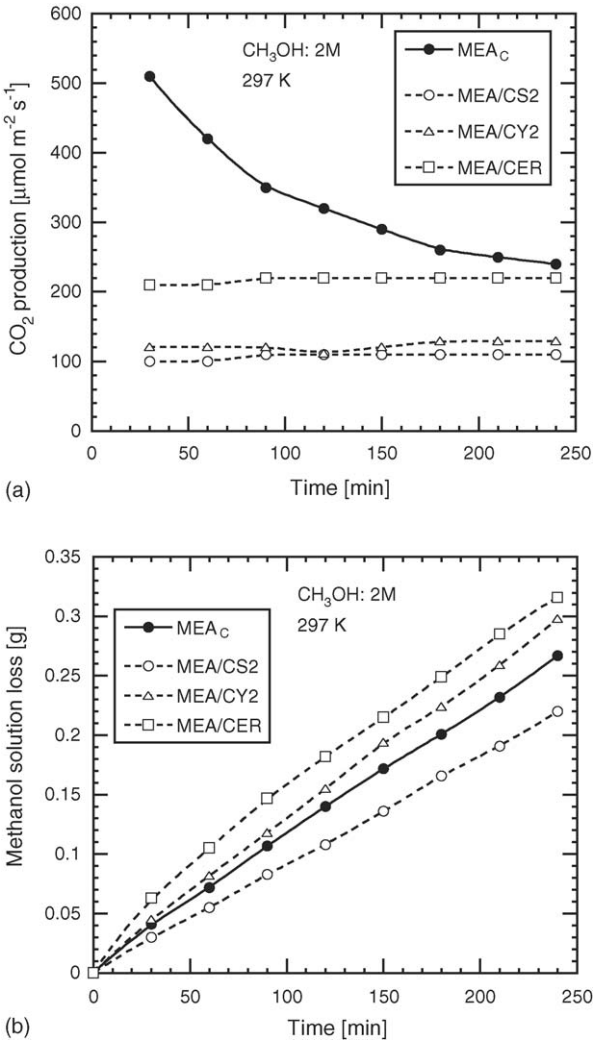

Fig. 2. Variations in (a) CO_2 production rate and (b) methanol solution loss with different porous materials at 2 M.

4. Results and discussion

4.1. CO_2 production rate and loss of the total solution

Fig. 2(a) shows the CO_2 production rate measured for MEA_C, MEA/CS2, MEA/CY2 and MEA/CER at the methanol concentration of 2 M, at 297 K. The CO_2 production rate for the conventional MEA, MEA_C, was greater than that for the MEAs with the porous plate, especially at the initial time. At 25 min, the CO_2 production rate for the MEA_C was three to five times greater than that for the MEAs with the porous plate. The production rate for the MEAs with the porous plate was different from each other according to the type of porous plate. It should be noted that CO_2 production rate when using the porous plate was nearly constant during the measurement, whereas the rate for the conventional MEA was initially high and decreased with time. Although the CO_2 production rate did not accurately agree with the rate of the methanol crossover due to the −10% to −15% error in the mass balance, it roughly indicated that the rate of MCO for each MEA. Hence, it was clear that the porous plate

significantly reduced the methanol crossover and constantly stabilized the crossover rate for a long time, and also, the degree of reduction in the methanol crossover depended on the properties of the porous plate.

Fig. 2(b) shows the weight loss of the cell holder with time for the cases shown in Fig. 2(a). The weight loss was due to the crossover of methanol and water from the reservoir to the oxygen chamber followed by the vaporization that transferred the solution out of the chamber with the oxygen flow. The methanol solution loss increased with the increasing time in all cases. Here, it should be noted that the order of the rate of the loss did not agree with the order of the CO_2 production rate shown in Fig. 2(a). This suggested that the rate of the methanol crossover did not coincide with the rate of the water permeation.

Figs. 3 and 4 show the CO_2 production rate and the weight loss at 4 and 8 M, respectively. At 4 M, as shown in Fig. 3(a) and (b), nearly the same trend as that shown in Fig. 2 was obtained, but both the CO_2 production rate and the loss of the methanol solution increased with the increase the methanol concentration from 2 to 4 and 8 M. With the increasing concentration of

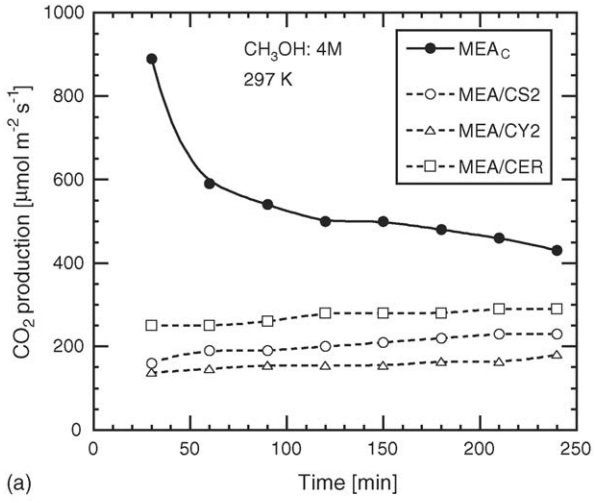

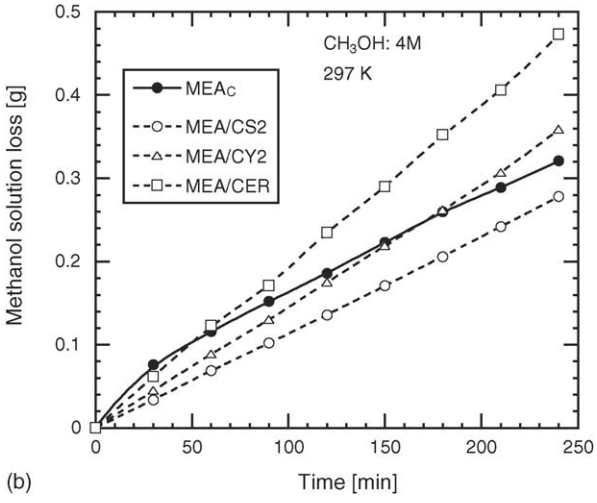

Fig. 3. Variations in (a) CO_2 production rate and (b) methanol solution loss with different porous materials at 4 M.

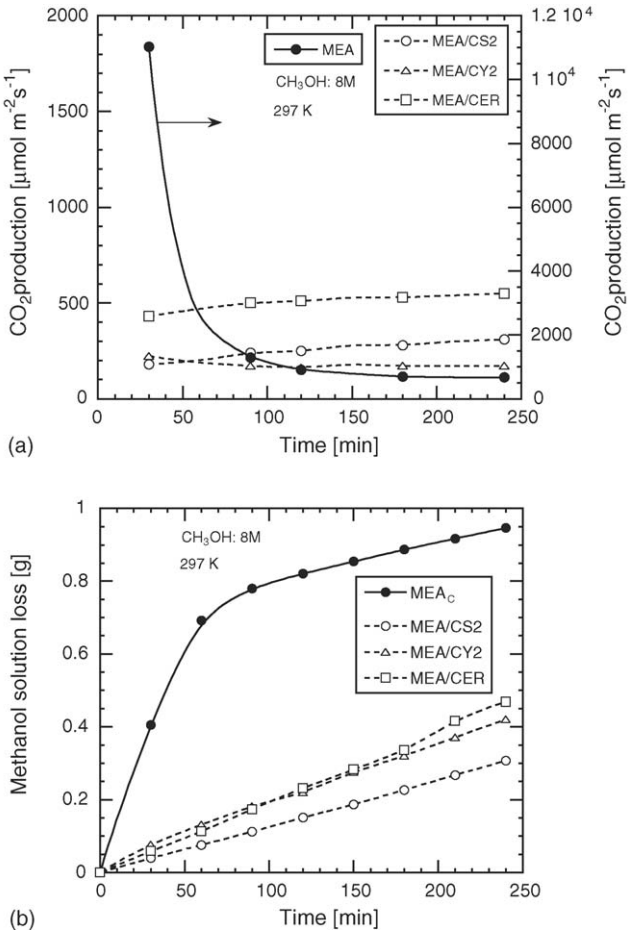

Fig. 4. Variations in (a) CO_2 production rate and (b) methanol solution loss with different porous materials at 8 M.

methanol in the reservoir, the methanol flux increased according to Eq. (6). The difference in the methanol concentration of the solution between both surfaces of the porous plate increased with the increasing concentration in the reservoir.

When the methanol concentration was as high as 8 M, the methanol crossover for the conventional MEA, MEA_C, was significantly increased from that at 4 and 2 M. The production rate of CO_2 for the MEA_C was 30–60 times higher compared to that of the MEA with the porous plates as shown in Fig. 4(a). This was caused by an increase in the temperature of the MEA as shown in the next section. On the other hand, in the case of the MEAs with the porous pate, the rate of the methanol crossover remained low and constant with time.

4.2. *Effect of using the porous plate on cell temperature*

Fig. 5(a)–(c) shows the temperature of the cell in the measurement of the CO_2 production rate for each MEA, i.e., MEA_C, MEA/CS2 and MEA/CER, at 2, 4 and 8 M, respectively. In case of the MEA_C, the temperature increased from 297 to 306, 317 and 383 K, during 5–15 min at 2, 4 and 8 M, respectively, then decreased with time. Whereas, in the case of MEA/CS2 and MEA/CER, the temperatures slightly increased and the change at the end of the measurement was 2 and 6 K, respectively,

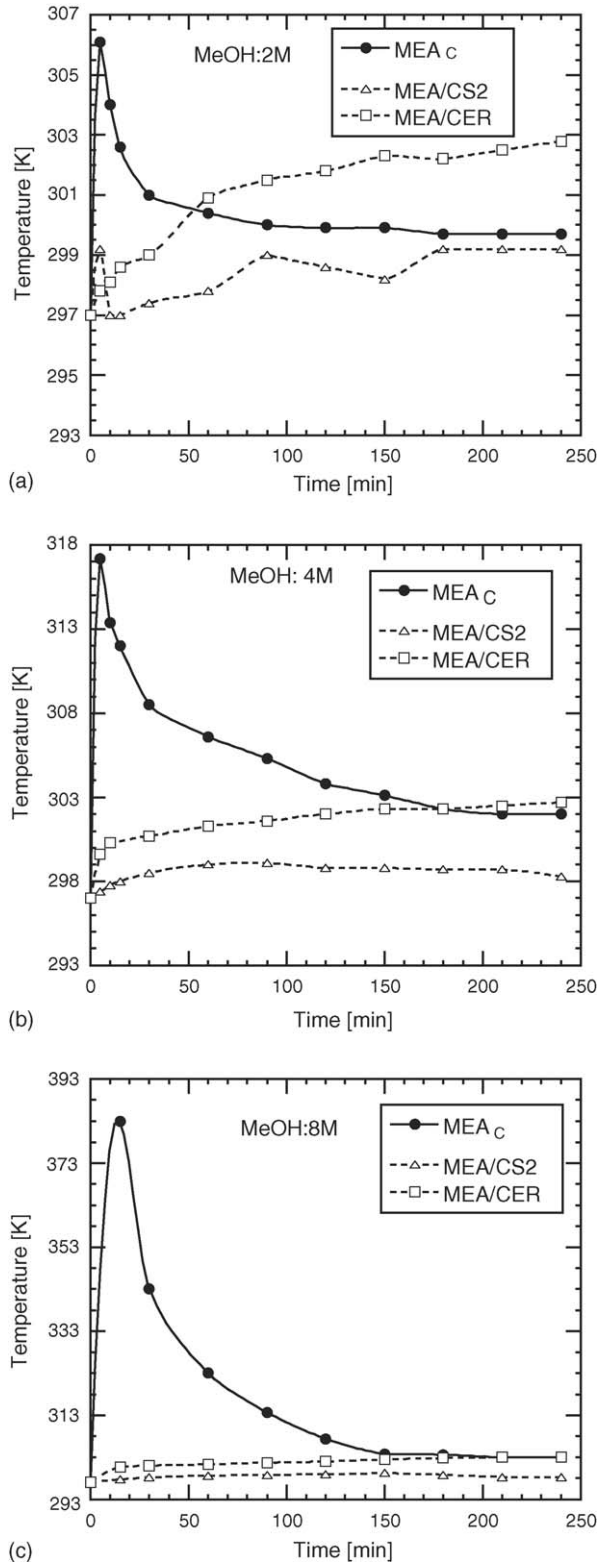

Fig. 5. Effect of using different porous plates on cathode temperature at different methanol concentrations of (a) 2 M, (b) 4 M, and (c) 8 M.

regardless of the methanol concentration. These temperature profiles were consistent with the variations in the production rate of CO_2 shown in Figs. 2–4. The consistency between them was reasonable, because the increase in temperature was caused

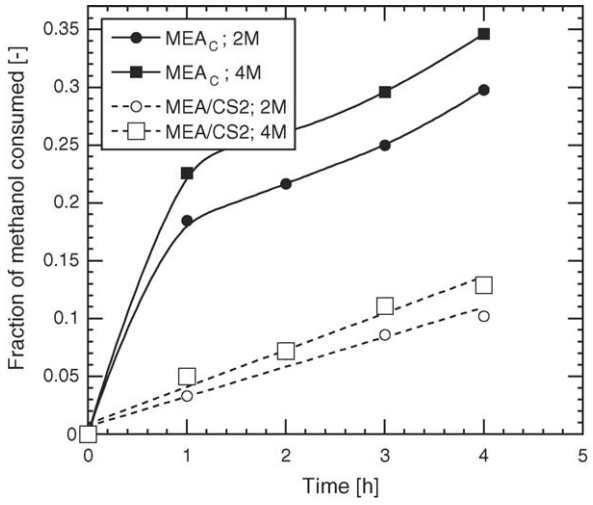

Fig. 6. Effect of using porous plate on methanol consumption at different methanol concentrations of 2 and 4 M.

by the oxidation of the methanol that permeated to the cathode. It should be noted that the temperature at 8 M for the conventional MEA reached 383 K that is close to the glass transition temperature of Nafion. Such a high temperature resulted from the methanol crossover being out of control by acceleration by the increase in temperature, and it may cause significant damage to the microstructure of the MEA. This pointed out that such a high methanol concentration cannot be used during practical operation of DMFC with the conventional MEA. As a result of the uncontrollable methanol crossover, the loss of methanol fed to the reservoir significantly increased.

Fig. 6 shows the fraction of the methanol consumed in the reservoir for every 1 h interval for the MEA_C and MEA/CS2 at 2 and 4 M. It was clearly shown that the consumption of methanol for the MEA_C was several times higher than that for MEA/CS2 in the first 1 h where the uncontrollable methanol crossover occurred as shown in Figs. 2, 3 and 5. In case of the MEA_C, a large fraction of methanol was lost during the initial time due to the initial high methanol concentration and decreased with increasing time because of a decrease in the methanol concentration during the time. However, in the case of using the porous plate, the methanol crossover was controlled by the resistance for mass transfer by the porous plate, and it resulted in a small and linear increase in the consumed fraction with increasing time. As shown above, it was clear that the MEA with the porous plate provided an important function of controlling the methanol crossover rate.

4.3. Effect of different properties of porous plate on methanol crossover

Fig. 7 shows the effect of the membrane thickness on the methanol flux and the water flux measured for the MEA with (b) and without (a) a porous plate. When a porous plate was not used as the support, Fig. 7(a), the methanol flux decreased in the order of Nafion 112, 115 and 117, i.e., in the order with the increasing thickness of the membrane, suggesting that the mass transport through the membrane controlled the methanol

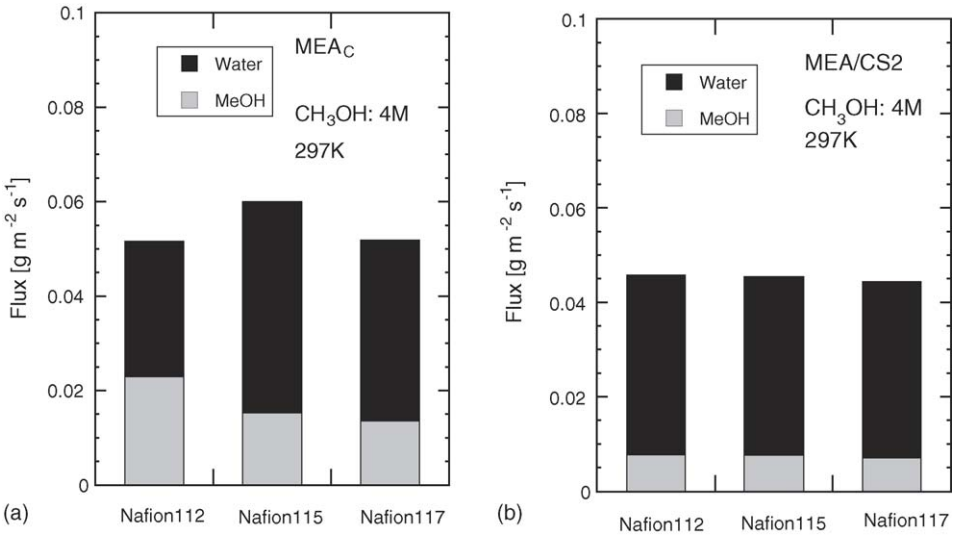

Fig. 7. Effect of membrane thickness on the methanol and water fluxes for the conventional MEA and MEA with a porous plate.

flux. On the other hand, the methanol flux and also the water flux for the MEA with the porous plate were not affected by the membrane, suggesting that these fluxes were not controlled by the membrane, but by the porous plate when the porous plate was used.

Fig. 8 shows the methanol flux and water flux measured for the different MEAs with and without a porous plate at 2, 4 and 8 M. It was clearly shown that the methanol flux was reduced at the MEAs with a porous plate compared to that at the MEA$_C$. It was also found that the methanol flux almost proportionally increased with the increasing methanol concentration as suggested by Eq. (6), except for the MEA$_C$ case at 8 M. The exceptional case, MEA$_C$ at 8 M, must be affected by the significant increase in temperature at the initial time as described above. Not only the methanol flux, but also the water flux was dependent on the properties of the porous plate. Therefore, we

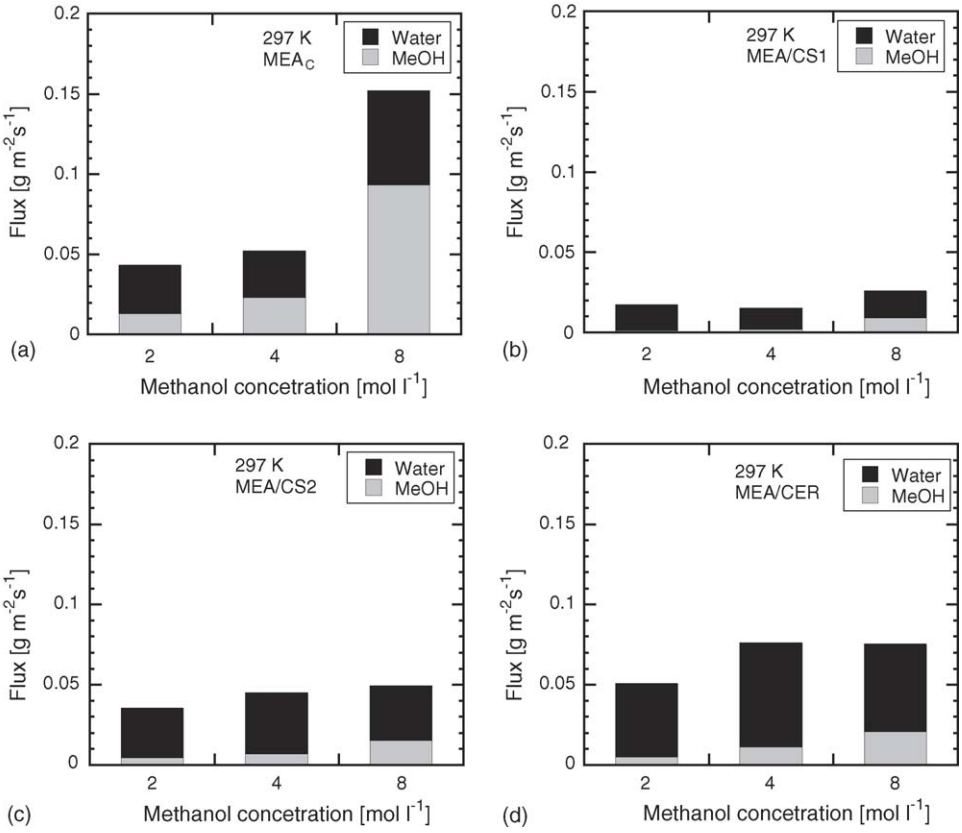

Fig. 8. Methanol and water fluxes for MEAs with and without porous materials: (a) MEA$_C$, (b) MEA/CS1, (c) MEA/CS2, and (d) MEA/CER.

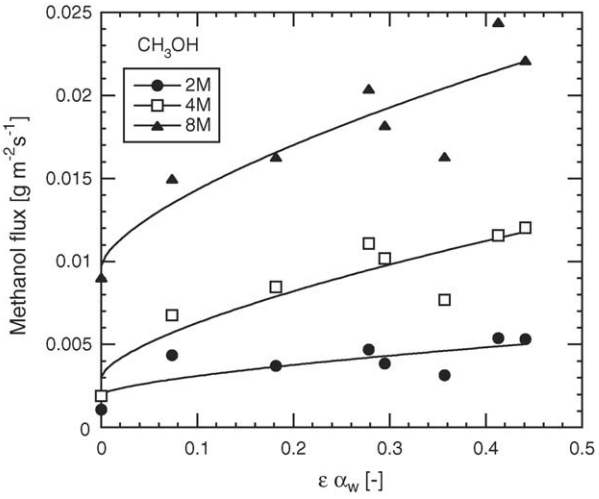

Fig. 9. Effect of $\varepsilon\alpha_w$ on the methanol flux.

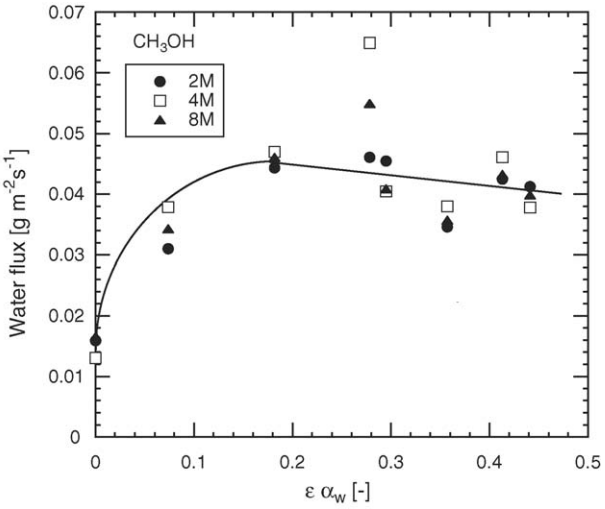

Fig. 10. Effect of $\varepsilon\alpha_w$ on the water flux.

investigated the property that affected the methanol flux for the porous plates used.

Fig. 9 shows the relationship between the methanol flux and the product of the porosity, ε, and the water absorptivity, α_w, for all of the MEAs with the porous plate shown in Table 1. A strong correlation could be observed between the methanol flux and the product, $\varepsilon\alpha_w$, as shown in the figure, but not between the methanol flux and the porosity, suggesting that the methanol transport was controlled by the diffusion through the flood pore with the solution as assumed in Eq. (8). The curves drawn in the figure were the results of a curve fitting for the data with the function: $a + b\,(\varepsilon\alpha_w)^{2/3}$, where a and b were constants, based on Eq. (8). The methanol flux increased with the increasing $\varepsilon\alpha_w$ and the methanol concentration. On the other hand, the methanol flux obtained for MEA_C was 0.0125, 0.0230 and 0.0927 g m^{-2} s^{-1} at 2, 4 and 8 M, respectively. The reduction in the methanol flux for the MEA with the porous plate having $\varepsilon\alpha_w = 0$ and 0.2 was calculated as around 1/10 and 1/5, respectively, to that for the conventional MEA at the methanol concentrations used in this study.

Fig. 10 shows the relationship between $\varepsilon\alpha_w$ and the water flux at different methanol concentrations. The water flux increased with the increasing $\varepsilon\alpha_w$ up to a definite value then it slightly decreased. It would be controlled by the evaporation rate of the solution at the cathode as assumed in the theoretical section. For the conventional MEA without a porous plate, the MEA_C, the obtained water flux was 0.0303, 0.0278 and 0.0593 g m^{-2} s^{-1} at 2, 4 and 8 M, respectively. The high water flux at 8 M would be caused by the high temperature shown in Fig. 4(a). Where as, similar and relatively low water fluxes for MEA_C at 2 and 4 M, compared to 0.045 g m^{-2} s^{-1} for the MEA with the porous plate, would result from the total flux controlled by the evaporation of the solution transported to the cathode as assumed in the theoretical section.

The total flux that was the sum of the methanol flux and the water flux for the different MEAs with the porous plate are plotted in Fig. 11, showing the total fluxes at 2 and 4 M for the MEA_C as the dotted lines. When $\varepsilon\alpha_w$ was over 0.2, the total flux became constant for the MEAs with the porous plate and it was also similar to that for the MEA without the porous plate. This supported the assumption that the total flux was controlled by the rate of evaporation of the permeated solution at the cathode as described in the theoretical section. It is known that the evaporation rate of water from a surface of a porous material become constant over a certain water content, because the lateral diffusion within a boundary layer allows the vapor pressure to equilibrate [36]. Due to this phenomenon, the water flux would be constant at an $\varepsilon\alpha_w$ over 0.2. During fuel cell operation, the water content in the membrane is very important, because the ionic conductivity of the membrane is directly related to the water content and temperature. On the other hand, excessive water at the cathode may cause flooding, i.e., liquid water accumulated at the cathode prevents oxygen access to the reaction sites. The water content in the membrane should be properly controlled during fuel cell operation.

Fig. 12 shows the relationship between the valuable of $\varepsilon\alpha_w$ and the degree of methanol separation defined by the methanol

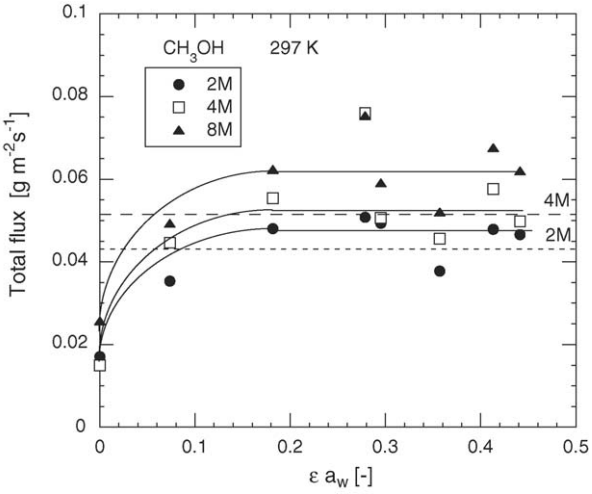

Fig. 11. Effect of $\varepsilon\alpha_w$ on the total flux.

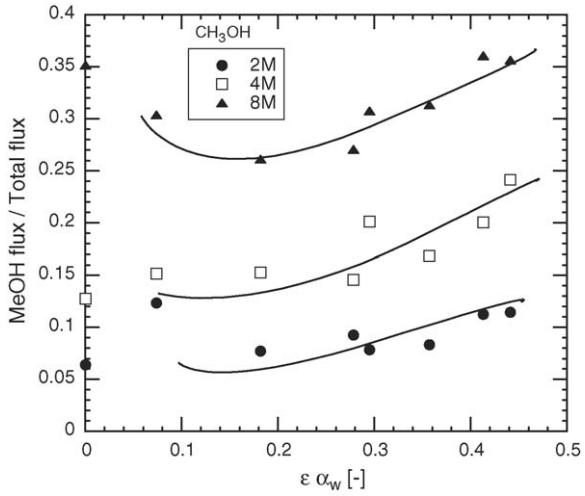

Fig. 12. Effect of $\varepsilon\alpha_w$ on the separation.

flux divided by the total flux. When the degree of separation was low, it means that the porous plate strongly controlled the methanol flux compared to the water flux. This figure showed that there was an optimum value for $\varepsilon\alpha_w$ at around $\varepsilon\alpha_w = 0.2$ where the degree of separation shows a minimum at a high methanol concentration. The degree of separation calculated for the conventional MEA was 0.292, 0.453 and 0.670 at 2, 4 and 8 M, respectively. It clearly showed that the degree of separation for the MEA with the porous plate was much smaller, 1/2–1/6, than that for the conventional MEA.

Fig. 13 shows the relationship between the change in the methanol concentration, C/C_0, and the loss of the solution, W/W_0, at different MEAs, where C and W are the methanol concentration and the weight of the solution, respectively, remaining in the reservoir after the 4 h crossover experiment, and C_0 and W_0 are the initial values. The plots for MEA_C are located at the lower positions in C/C_0 and also W/W_0 compared to the plots for the MEAs with the porous plate, whereas, the plots for the MEAs

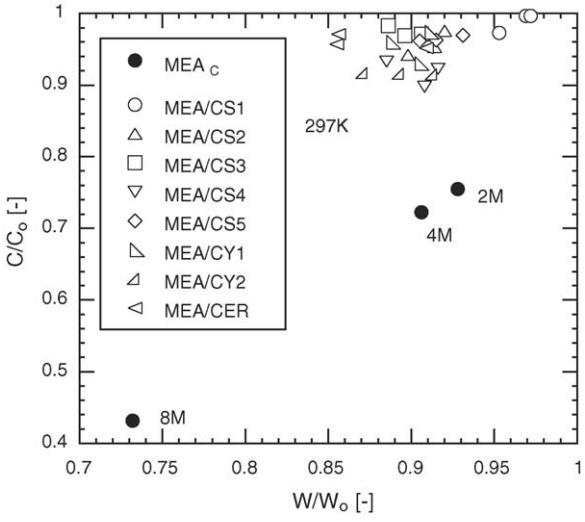

Fig. 13. Relationship between the decrease in the weight and that in the methanol concentration for the solution remaining in the reservoir during the 4 h crossover experiment.

with the porous plate, including that at 2, 4 and 8 M, located in the domain with $C/C_0 > 0.9$ and $W/W_0 > 0.85$ in the figure. This means that the methanol is preferentially transported through the conventional MEA, and it was controlled by the porous plate. As shown in Eq. (5), the methanol flux J_M was accelerated by the increase of the diffusion flux through the membrane J_{DM} due to the large difference in the methanol concentration between the anode and cathode for the conventional MEA. The value of J_{DM} was reduced for the MEA with the porous plate by reducing methanol concentration at the anode surface resulting in a reduced driving force for J_{MD} by the diffusion resistance of the porous plate. Hence, C/C_0 was never greater than 1 in all cases.

4.4. Effect of surrounding temperature on MCO

Fig. 14 shows the effect of the surrounding temperature ranging between 297 and 323 K on the total flux for the MEA_C and MEA/CS2. The total flux increased with the increasing temperature showing the minus slope on the Arrhenius plot for both cases of the MEA_C and MEA/CS2. The plots showed a straight line within the temperature range measured at 2 and 4 M for

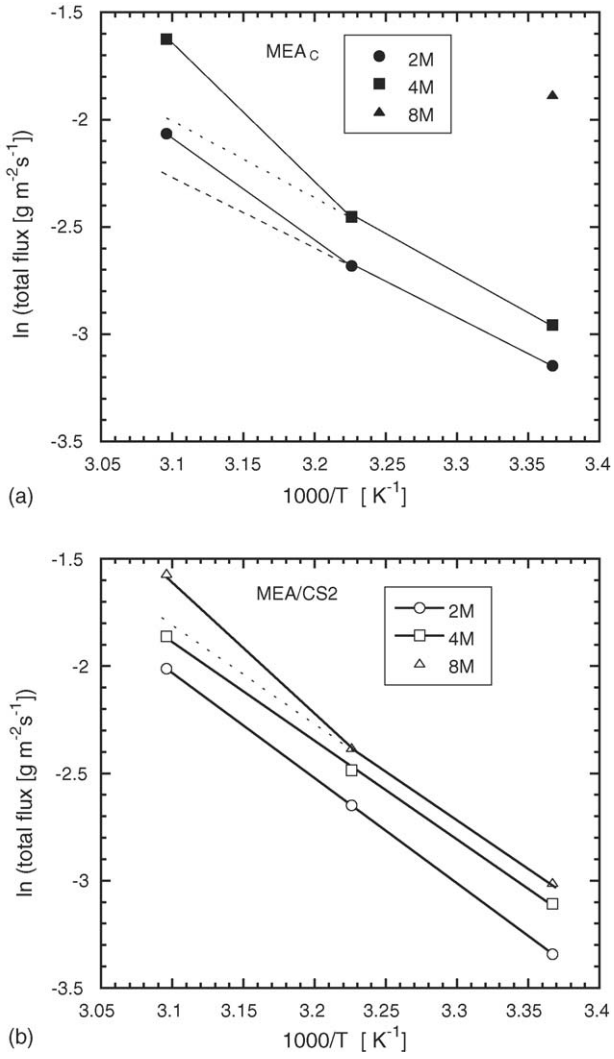

Fig. 14. Arrehenuis plot for total flux in case of (a) MEA_C and (b) MEA/CS2.

MEA/CS2, as shown in Fig. 14(b). The activation energy calculated for both cases was 39 kJ mol^{-1} which almost agreed with the latent heat of vaporization of water, 44 kJ mol^{-1}. This suggested that the total flux was controlled by the evaporation rate of water at the cathode as mentioned in the theoretical consideration with Eqs. (2) and (4), noting that the vapor pressure of the cathode gas, p_a, in the equation was negligibly small in this measurement. At 323 K and 8 M for MEA/CS2, the total flux was plotted above the straight line that was for the plots at low temperatures. This would be because the actual temperature of the cell was higher than that of the surrounding one due to the effect of the high methanol crossover at this condition. A similar tendency was observed for the conventional MEA, MEA$_C$, at 2 and 4 M as shown in Fig. 14(a). In the case of MEA$_C$, the effect of the methanol crossover on the actual temperature of the cell was significant even at the low concentration of 2 M. Hence, the relationship between the total flux and the surrounding temperature did not reflect the actual relationship between the flux and the cell temperature. The experiments for the higher temperatures, 310 and 323 K, at 8 M were not conducted because it was uncontrollable.

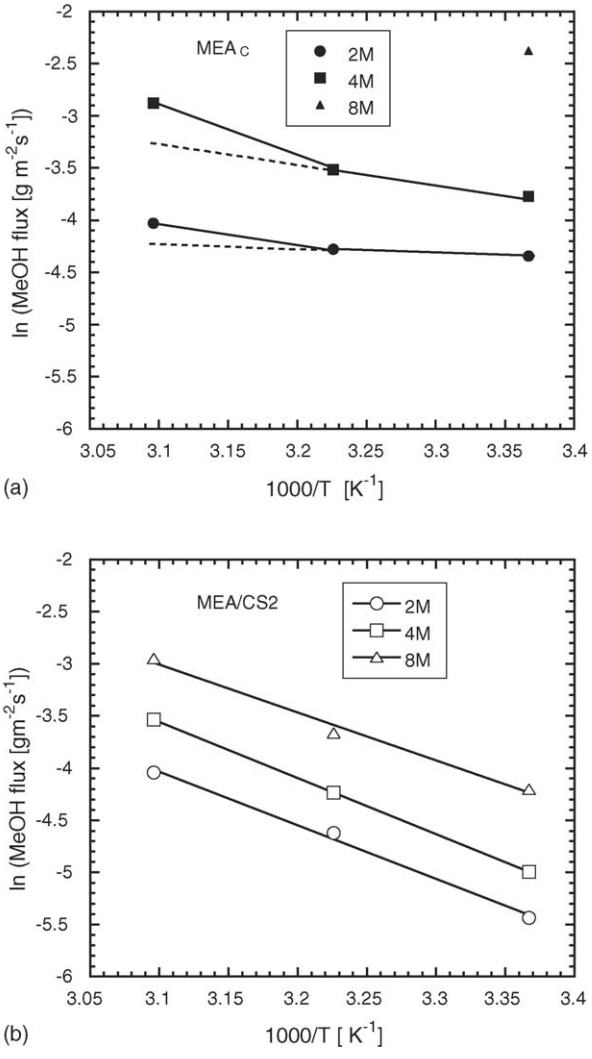

Fig. 15. Arrehenuis plot for methanol flux in case of (a) MEA$_C$ and (b) MEA/CS2.

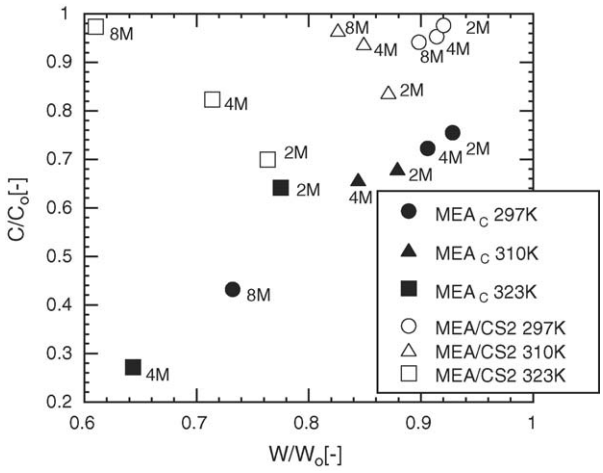

Fig. 16. Relationship between the decrease in the weight and that in the methanol concentration for the solution remaining in the reservoir during the 4 h crossover experiment. Comparison between MEA$_C$ and MEA/CS2 at different temperatures and methanol concentrations.

Fig. 15 shows the effect of temperature on the methanol flux for both the MEA$_C$ and MEA/CS2. The activation energies at different methanol concentrations for MEA/CS2 were 42.7, 44.7 and 38.2 kJ mol^{-1} at 2, 4 and 8 M, respectively. These values were much higher than that calculated for the diffusion. This confirmed that the methanol transport through the MEA was by diffusion and convection flow from the anode to the cathode as given in Eq. (5), and the convective flow was accelerated by the increase in the surrounding temperature as mentioned above. Based on this consideration, the blocking of the methanol transport by the porous plate based on the diffusion resistance mechanism would be reduced under the condition of high temperature and high methanol concentration, because the methanol flux by the diffusion would be relatively low to that due to the convective flow driven by the evaporation of water at the cathode.

Fig. 16 shows the relationship between the separation and the loss for the cases measured at different surrounding temperatures for the MEA$_C$ and MEA/CS2. The separation of methanol by the porous plate was still effective at these temperatures, although the loss of the total solution relatively increased as the temperature increased for the cases with MEA/CS2.

All the above experiments were conducted under open circuit conditions. However, the methanol crossover under closed circuit conditions is also important. When the circuit is closed and current flowed, carbon dioxide is produced at the anode. The carbon dioxide must be transported to the outside mainly through the porous plate when the porous plate is used. The authors are currently investigating the methanol crossover at MEAs with the porous plate under closed circuit conditions which will be reported elsewhere in the future.

5. Conclusions

Methanol crossover in a passive DMFC using a porous plate as a support had been studied under open circuit conditions using different porous plates with different structures and different

water absorptivities at different methanol concentrations and temperatures. The following conclusions were drawn.

The porous plates controlled and reduced the methanol crossover. As the material of the porous plate, both the porous carbon plate and the porous Al_2O_3 plate were useful. The mechanism of reducing the methanol crossover could be explained by the controlling the diffusion of methanol through the porous plate which reduced the methanol flux. As the properties of the porous plate that affect the methanol flux, the porosity, water absorptivity and others involved in Eq. (8), were predicted, which were confirmed by experiment. The methanol flux and water flux could be expressed as a function of the products of the porosity and the water absorptivity, $\varepsilon\alpha_w$. The methanol flux increased with the increasing $\varepsilon\alpha_w$ and the methanol concentration. The water flux increased with the increasing $\varepsilon\alpha_w$ to a certain value of $\varepsilon\alpha_w$ and then slightly decreased, and was not affected by the methanol concentration. As a result of reducing the methanol crossover, the temperature of the cell was constantly controlled without causing an uncontrollable temperature increase that was observed for the conventional MEA. Also, a considerable amount of methanol loss due to the uncontrollable temperature increase was neglected for the MEAs with the porous plate. The total flux for the MEAs with the porous plate measured at different surrounding temperatures showed an activation energy similar to that of the latent heat of vaporization of water, suggesting that the evaporation rate controlled the total flux.

Acknowledgments

The authors acknowledge the New Energy and Industrial Technology Development Organization (NEDO) for their financial support of this study, and Mitsubishi Pencil Co., Ltd., for the preparation and gift of the porous carbon plate.

References

[1] H. Chang, J.R. Kim, J.H. Cho, H.K. Kim, K.H. Choi, Solid State Ionics 148 (2002) 601–606.
[2] A. Blum, T. Duvdevani, M. Philosoph, N. Rudoy, E. Peled, J. Power Sources 117 (2003) 22–25.
[3] D. Kim, E.A. Cho, S.A. Hong, I.H. Oh, H.Y. Ha, J. Power Sources 30 (2004) 172–177.
[4] A.S. Arico, S. Srinivasan, V. Antonucci, Fuel Cells 1 (2001) 133–161.
[5] T. Schultz, K. Su Zhou, Sundmacher, Chem. Eng. Technol. 24 (2001) 1223–1233.
[6] S. Surampudi, S.R. Narayanan, E. Vamos, H. Frank, G. Halpert, A. LaConti, J. Kosek, G.K. Surya Prakash, G.A. Olah, J. Power Sources 47 (1994) 377–385.
[7] M.K. Ravikumar, A.K. Shukla, J. Electrochem. Soc. 143 (1996) 2601–2606.
[8] J.T. Wang, S. Wasmus, R.F. Savinell, J. Electrochem. Soc. 143 (1996) 1233–1239.
[9] E. Peled, T. Duvdevani, A. Aharon, A. Melman, Electrochem. Solid State Lett. 3 (2000) 525–528.
[10] M.V. Fedkin, X. Zhou, M.A. Hofmann, E. Chalkova, J.A. Weston, H.R. Allcock, S.N. Lvov, Mater. Lett. 52 (2002) 192–196.
[11] T. Yamaguchi, M. Ibe, B.N. Nair, S. Nakao, J. Electrochem. Soc. 149 (2002) A1448–A1453.
[12] M.L. Ponce, L. Prado, B. Ruffmann, K. Richau, R. Mohr, S.P. Nunes, J. Membr. Sci. 217 (2003) 5–15.
[13] A.S. Arico, P. Creti, P.L. Antonucci, V. Antonucci, Electrochem. Solid State Lett. 1 (1998) 66–68.
[14] C. Yang, S. Srinivasan, A.S. Arico, P. Creti, V. Baglio, V. Antonucci, Electrochem. Solid State Lett. 4 (2001) A31–A34.
[15] N. Jia, M.C. Lefevre, J. Halfyard, S. Qi, P.G. Pickup, Electrochem. Solid State Lett. 3 (2000) 529–531.
[16] I.J. Hobson, H. Ozu, M. Yamaguchi, M. Muramatsu, S. Hayase, J. Mater. Chem. 12 (2002) 1650–1656.
[17] W.C. Choi, J.D. Kim, S.I. Woo, J. Power Sources 96 (2001) 411–414.
[18] S.R. Yoon, G.H. Hwang, W.I. Cho, I.-H. Oh, S.-A. Hong, H.Y. Ha, J. Power Sources 106 (2002) 215–223.
[19] Y.K. Xiu, K. Kamata, T. Ono, K. Kobayashi, T. Nakazato, N. Nakagawa, Electrochemistry 73 (2005) 67–70.
[20] N. Nakagawa, K. Kamata, A. Nakazawa, M. Ali Abdelkareem, K. Sekimoto, Electrochemistry 74 (2006) in press.
[21] G.Q. Lu, C.Y. Wang, T.J. Yen, X. Zhang, Electrochim. Acta 49 (2004) 821.
[22] Z. Guo, Y. Cao, J. Power Sources 132 (2004) 86–91.
[23] J. Liu, G. Sun, F. Zhao, G. Wang, G. Zhao, L. Chen, B. Yi, Q. Xin, J. Power Sources 133 (2004) 175–180.
[24] T. Shimizu, T. Momma, M. Mohamedi, T. Osaka, S. Sarangapani, J. Power Sources 137 (2004) 277–283.
[25] H. Qiao, M. Kunimatsu, T. Okada, J. Power Sources 139 (2005) 30.
[26] Q. Ye, T.S. Zhao, J. Power Sources 147 (2005) 196–202.
[27] R. Chen, T.S. Zhao, J. Power Sources 152 (2005) 122–130.
[28] J. Liu, T. Zhao, R. Chen, C.W. Wong, Fuel Cells Bull. February (2005) 12–17.
[29] B. Kho, I. Oh, S. Hong, H.Y. Ha, Fuel Cells Bull. September (2004) 11–14.
[30] J.G. Liu, T.S. Zhao, R. Chen, C.W. Wong, Electrochem. Commun. 7 (2005) 288.
[31] B. Kho, I. Oh, S. Hong, H.Y. Ha, Electrochim. Acta 50 (2004)781.
[32] C.Y. Chen, P. Yang, J. Power Sources 123 (2003) 37–41.
[33] B. Bae, B.K. Kho, T. Lim, I. Oh, S. Hong, H.Y. Ha, J. Power Sources 158 (2006) 1256–1261.
[34] J.G. Liu, T.S. Zhao, Z.X. Liang, R. Chen, J. Power Sources 153 (2006) 61–67.
[35] R. Chen, T.S. Zaho, J.G. Liu, J. Power Sources 157 (2006) 351–357.
[36] M. Suzuki, S. Maeda, J. Chem. Eng. Japan 1 (1968) 26–31.